# SUPPLEMENTARY MATERIAL

## Prediction of surgical outcomes in normal pressure hydrocephalus by magnetic resonance elastography

### *A. Image Processing*

Tissue probability maps were segmented from a T1-weighted anatomical image. These maps were computed by unified segmentation in SPM12 using the Mayo Clinic Adult Lifespan Template (MCALT)[1, 2]. To reduce any misregistration errors between the maps and the MRE data, segmentation was run on the anatomical T1-weighted image and the T2-weighted MRE magnitude image together after rigid body registration and re-slicing of the T1-weighted image into MRE space. A brain mask was computed to retain voxels where the combined probability of white matter and gray matter tissues was greater than that of CSF. A lobar atlas was warped into MRE space for each participant using the inverse deformation field computed during segmentation.

Stiffness and damping ratio maps were computed from the MRE data using a previously described neural network inversion (NNI)[3]. Training data were generated with a finite difference model with randomly distributed and spatially shaped mechanical properties to relax the tissue homogeneity assumption. Displacement images were filtered to reduce interslice phase discontinuities[4], and then unwrapped by a graph cut method[5]. Property estimation was then performed separately in six regions to perform inversion across displacement discontinuities caused by major dural folds or relatively large CSF compartments. Within each region (computed as the intersection of the relevant lobar atlas regions and the brain mask), the curl was computed with adaptive methods to eliminate the effects of longitudinal waves[4]. In voxels located within multiple regions (e.g., corpus callosum), the mean value of each regional estimate was used in the final property maps. This process was repeated to compute the two mechanical property maps, stiffness, and damping ratio.

Mechanical property maps were then transformed into MCALT space for further analysis using the previously computed deformation fields. Property maps were resampled by nearest neighbor interpolation to avoid the introduction of underestimates at the edge of the brain parenchyma.

### *B. Leave one out pattern analysis*

Pattern analysis presented in this study was based on calculating the spatial correlation of a corrected mechanical property map of individuals compared to reference maps from different contrasts. The averaged spatial correlation score was calculated for stiffness and damping ratio maps separately using Pearson's linear correlation coefficient in MATLAB 2017b with default parameters. The flow chart for the process is shown on the left panel of Figure 1 of the main text. To calculate the correlation score, an

individual's stiffness or damping ratio maps are held aside and the maps of remaining participants, except for one other group, were used for voxel-wise modeling. For example, in the Congenital vs Control pattern analysis shown in Figure S1 (a), the control group was excluded in the modeling creating the required contrast. Consequently, congenital group's mechanical correlates to the anatomical features that are absent in control group became the reference map. This allows the extraction of patterns specific to the congenital group that are absent in the Control group. Similarly, for the rest of the plots in Figure S1, the first group in the title is the group whose features comprise the reference map excluding the features present in the second group. As another example, Congenital vs Ventric in Figure S1 (c) shows the extraction of features present in the congenital group other than ventriculomegaly since both groups have that feature in common.

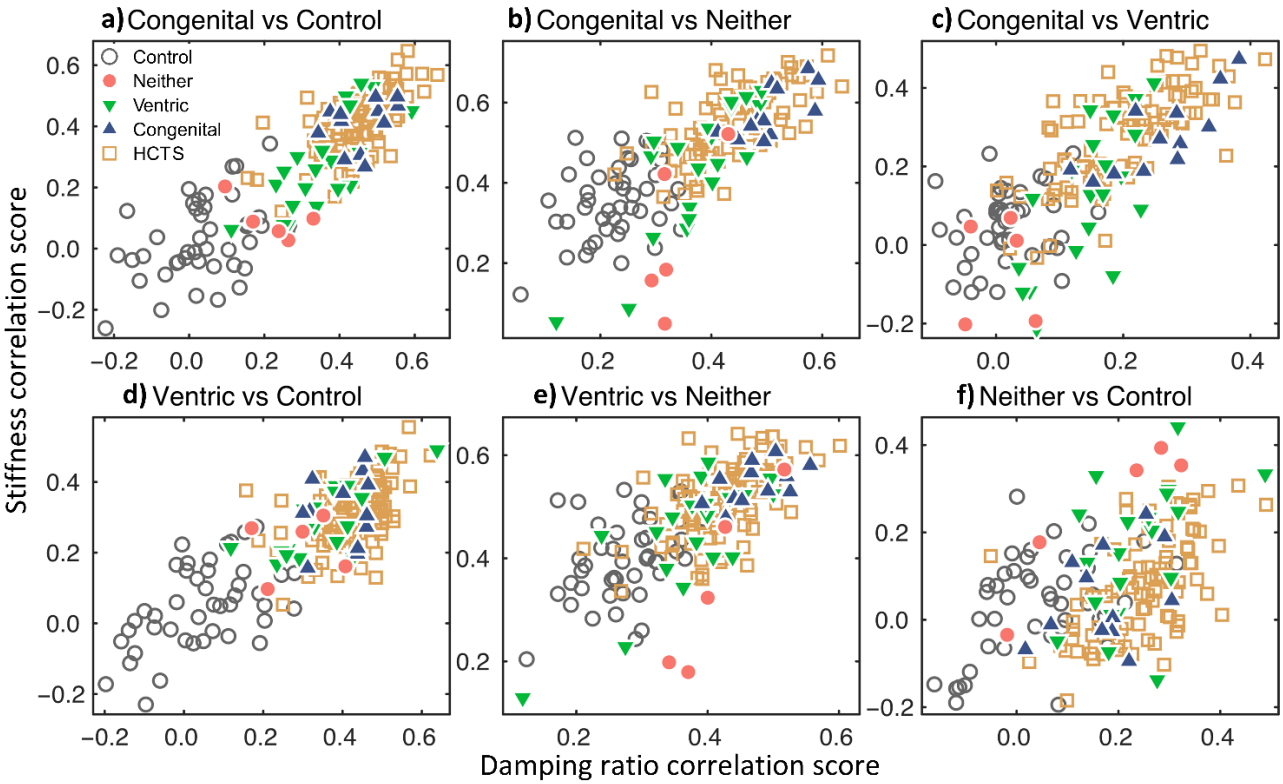


Figure S1. (a) Correlation scores for congenital and control are separated distinctly into two clusters. The features of ventriculomegaly, diffusely narrowed cerebral sulci, and presence of aqueductal stenosis or web were extracted in the process as the controls do not have such features. (b) Cases from congenital and neither groups were separated further compared to (a), but due to fewer cases and the lack of exact feature definition of the neither group, it is not possible to state the features being extracted. (c) Congenital vs Ventric extract features of diffusely narrowed cerebral sulci and the presence of aqueductal stenosis or web since these features are absent in Ventric cases. (d) Ventric vs Control contrast extracted the feature of ventriculomegaly, and since most of the NPH phenotypes have ventriculomegaly, there is a greater separation between the controls and all NPH cases compared to all the other plots. (e-f) Ventric vs Neither and Neither vs Control feature extractions are not well defined due to the confounding nature of cases in the neither group.

Before the calculation of the spatial correlation, the mechanical property maps of individuals were corrected for age, gender, and scanner related effects. Such corrections are necessary as studies have demonstrated that the viscoelastic properties of the brain are affected by aging and gender differences.

We also corrected for the scanner effects since scanners from two different vendors were used. After correcting an individual's viscoelastic maps, correlation scores were computed only over relevant (non-zero in maps being compared) voxels.

1. Ashburner J, Friston KJ. Unified segmentation. *Neuroimage* 2005;26:839-851
2. Schwarz CG, Gunter JL, Ward CP, et al. [P2–415]: The Mayo Clinic Adult Lifespan Template: Better Quantification Across The Lifespan. *Alzheimer's & Dementia* 2017;13:P792-P792
3. Scott JM, Arani A, Manduca A, et al. Artificial neural networks for magnetic resonance elastography stiffness estimation in inhomogeneous materials. *Med Image Anal* 2020;63:101710
4. Murphy MC, Huston J, 3rd, Jack CR, Jr., et al. Measuring the characteristic topography of brain stiffness with magnetic resonance elastography. *PLoS One* 2013;8:e81668
5. Bioucas-Dias JM, Valadão G. Phase unwrapping via graph cuts. *IEEE Trans Image Process* 2007;16:698-709